Oxidative Aromatic Substitutions: Hartree−Fock/Density Functional and ab Initio Molecular Orbital Studies of Benzene and Toluene Nitrosation[1]

Sergei Skokov and Ralph A. Wheeler*

Department of Chemistry and Biochemistry, University of Oklahoma, Norman, Oklahoma 73019

Received: May 12, 1998; In Final Form: September 23, 1998

Aromatic nitrosations are prototypes of a recently proposed reaction mechanism—oxidative aromatic substitutions—incorporating ground-state electron transfer prior to the substitution step. Ab initio MO and B3LYP hybrid Hartree−Fock/density-functional (HF/DF) calculations confirm that nitrosation proceeds through initial formation of intermediate electron donor−acceptor (EDA) π-complexes. Calculated π-complex geometries and energies agree qualitatively with experimental data and indicate the applicability of HF/DF methods for modeling EDA complexes. Subsequent transformation of (benzene−NO)$^+$ and (toluene−NO)$^+$ π-complexes into N-protonated nitroso-derivatives in B3LYP and MP2 calculations suggest an alternative to the currently proposed mechanism involving π-complex transformation into Wheland type σ-complexes (supported by CISD calculations). Kinetic analysis suggests the alternative mechanism is plausible and indicates that proton transfer from the N-protonated nitroso-derivatives to the medium would not be rate limiting. Instead, low nitrosation rates would be assigned to significant potential energy barriers for π-complex transformation into N-protonated nitroso-derivatives by a novel migratory insertion of nitrogen into the aromatic C−H bond. The insertion step exhibits a large, primary kinetic isotope effect of 11.5, in qualitative agreement with the isotope effect of 8.5 ± 2.4 previously measured for benzene nitrosation. The difference in B3LYP barrier heights for direct π-complex conversion to N-protonated nitroso-adducts would also account for the difference in substrate reactivities and regioselectivity in nitrosation reactions. Thus, the conflict between B3LYP and MP2 calculations vs the CISD results cannot be resolved by applying kinetic arguments and must await more definitive work.

The detection[2] and characterization[3−8] of π-complexes between nitrosonium cation (NO^+) and aromatics has opened an exciting new chapter in the chemistry of aromatic substitution reactions. Whereas aromatic substitutions were formerly categorized simply as electrophilic[9] or nucleophilic,[10,11] Kochi and co-workers[12,13] recently christened a new general mechanism "oxidative aromatic substitution" to describe reactions where electron transfer within an electron donor−acceptor (EDA) complex precedes the aromatic substitution step. Resolving the dichotomy between electrophilic and oxidative aromatic substitutions, equivalent to distinguishing between limiting cases of two-electron or one-electron processes, requires first establishing that EDA complexes are true reaction intermediates, a daunting experimental task. We undertook the current computational study to complement experimental efforts by addressing the roles of π- and σ-complexes, and particularly their electron donor−acceptor character, in the nitrosation by NO^+ of the representative benzene and toluene molecules. Before describing our computational methods and results, however, we place the work in context by discussing known features of EDA complexes between NO^+ and aromatics and describing experimental and computational evidence for their participation in aromatic substitution reactions.

Electron Donor−Acceptor Complexes in Aromatic Nitrosations

Although color changes evident upon mixing nitrosonium cation, NO^+, with aromatics were attributed to π-complex formation long ago,[2] the EDA complexes giving rise to the observed colors were thoroughly characterized only recently. A sketch of the 1:1 EDA

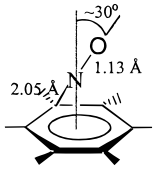

1

complex between NO^+ and hexamethylbenzene is shown in **1**, along with selected distances and angles from X-ray diffraction structures.[5,6] The NO^+ unit is located within 0.03 Å of the normal to the center of the ring in **1**, with an average N···C distance (2.05 Å) much less than the sum of van der Waals radii and a tilt angle of approximately 30° from the ring normal. Most remarkable are the N−O distances ranging from 1.13 Å (obtained by reacting hexamethylbenzene with $NO^+AsF_6^-$) to 1.36 Å (from reaction of hexamethylbenzene with $NO^+SbF_6^-$). Both measured distances fall nearer the experimentally measured bond distance for NO (1.15 Å)[14,15] than that for NO^+ (1.06 Å)[14] and imply partial reduction of the NO^+ moiety in the EDA complex. IR spectroscopy also implies that NO^+ is reduced in the EDA complex, since the measured NO stretching frequency of 1849 cm^{-1} is much closer to that of NO (1876 cm^{-1})[14,15] than that of NO^+ (2189 cm^{-1}).[14,15] Subsequent crystallographic and IR spectroscopic work with these and similar complexes[7] confirm the general features described here: N···C distances less than the sum of van der Waals radii, elongated NO distances, and NO stretching frequencies which are close to

10.1021/jp9822034 CCC: $18.00
Published on Web 05/11/1999

SCHEME 1

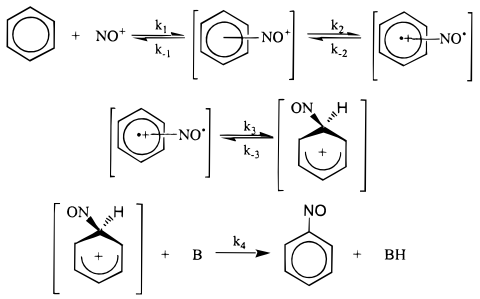

SCHEME 2

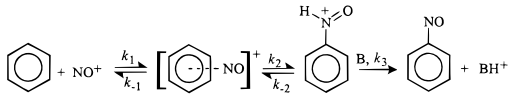

those for the neutral NO molecule, and much lower than that of NO^+. In addition, ^{13}C NMR resonances for methyl and aromatic carbons of hexamethylbenzene shift downfield from 17.0 and 133.2 ppm to 17.9 and 150.8 ppm, respectively, with added NO^+PF6^-.[7] These shifts are diagnostic of the increased cationic character of the aromatic ring and confirm the proposed ground-state electron transfer from the aromatics to NO^+ in their complexes.

Whereas N-nitrosation of aromatic amines has been prominent for years due to the diverse chemistry of the nitrosamine products, ranging from their potent carcinogenic activity[16] to their industrial conversion to azo dyes,[17] C-nitrosation only recently vaulted to prominence as the prototypical oxidative aromatic substitution reaction.[12,13] The putative EDA intermediates and electron-transfer steps in aromatic nitrosations[12,13] form a sharp contrast with aromatic nitrations, the most well-characterized electrophilic aromatic substitutions,[9,18] and the two reaction mechanisms are frequently contrasted. Whereas EDA complexes are isolable intermediates in nitrosations, to our knowledge EDA complexes of NO_2^+ have never been isolated, their existence is controversial, and even the identity of the actual nitrating agent is frequently unknown.[9,17,18] To remove complications caused by the presence of numerous nitrating and nitrosating agents (including NO^+, H_2ONO^+, NO_2^+, and $H_2ONO_2^+$) in aqueous nitrous acid, Kochi and co-workers performed careful kinetic studies of direct aromatic nitrosation by NO^+ in basic acetonitrile solutions.[12] The proposed mechanism for aromatic C-nitrosations that arose from their studies is illustrated in Scheme 1. According to Kochi et al.,[12] the aromatic first forms an EDA complex with NO^+, followed by electron transfer to form a complex of the aromatic radical cation with neutral NO. Subsequent rearrangement of the postulated π-complex to a σ-complex, or Wheland intermediate, is followed by deprotonation of the aromatic by base B to give the nitroso-aromatic product. The Wheland intermediate was not observed spectroscopically,[12] but large primary deuterium isotope effects are interpreted to imply rate-limiting deprotonation of a Wheland intermediate. Although the π-complex was also not definitively established as an intermediate in the reaction, support comes from gas-phase data obtained by Reents and Freiser[3,4] in spectroscopic studies of the decomposition of nitrosated benzene, $C_6H_6NO^+$, and substituent-protonated nitrosobenzene, $C_6H_5NOH^+$, through intermediate π-complexes. For gas-phase nitrosations, however, Reents and Freiser proposed the mechanism shown in Scheme 2 incorporating an N-protonated nitrosobenzene, but making no comment on any possible Wheland σ-complex.[3,4] Here, formation of the π-complex, reaction 1, proceeds without barrier, while formal insertion of NO into the carbon−hydrogen bond, reaction 2, encounters a significant barrier. No Wheland intermediate was detected and no experimental data are available concerning the location of the hydrogen on the NO moiety, but the hydrogen was presumed bonded to nitrogen based on previous MO calculations for HNO. The product formation step, reaction 3, is the proton transfer to the medium, and is usually considered irreversible. In solvent, a large deuterium kinetic isotope effect is observed as a common feature of aromatic nitrosation reactions[12,17,19] and has led to the conclusion, now widely accepted, that proton transfer to the medium is the rate-limiting step in aromatic nitrosations.[19]

Computational Background and Methods

Olefin−NO^+ complexes have been studied computationally several times,[20−22] but surprisingly little computational work has been published to address the mechanism of aromatic nitrosations and what has been published conflicts with experiment in important ways. Studies of aromatic nitrosation utilized the MINDO/3 semiempirical Hamiltonian and suggested a rather complex nitrosation mechanism[23] with two intermediate π-complexes and a Wheland σ-complex. The latter is reported to be only 2 kcal/mol below the energy barrier for reaction 2 of Scheme 2, too unstable to be easily observed in experiments. Yet, a large discrepancy between experimental and computed reaction energetics[23] indicates inadequacies of the simple MINDO/3 Hamiltonian for this particular problem.

Modeling partial electron transfer in chemical reactions is generally very difficult because a balanced treatment of closed- and open-shell systems requires including both dynamical and nondynamical correlation energy corrections.[24−26] Restricted Hartree−Fock (RHF) calculations favor closed-shell systems, semiempirical treatments such as MINDO/3 are biased toward the limiting case of diradical reactions paths, and unrestricted Hartree−Fock (UHF) must incorporate dynamical correlation energy corrections to provide even qualitatively correct results.[24,27] Computationally intensive MO methods such as multireference configuration interaction[28,29] or complete active space perturbation theory (CASPT2)[30−32] are necessary to provide a balanced treatment of two-electron, closed-shell paths and diradical, or open-shell mechanisms.

The computational requirements of CASPT2 and other post-Hartree−Fock MO methods can become extreme for large molecules, but methods based on density-functional theory (DFT) were designed to calculate dynamical correlation energies,[33−39] so they provide attractive alternatives that are computationally efficient[40,41] and provide a more balanced treatment of open- and closed-shell systems than low-level, post-HF methods.[42−44] Initial studies using DFT with nonlocal gradient corrections for bond dissociation energies[45−47] as well as singlet−triplet gaps in carbenes and related species[45−49] indicate that DFT can reproduce energy differences between closed-shell and open-shell species. Reaction energetics are superior to HF results and comparable to those of a second-order Møller−Plesset perturbation approximation (MP2) of electron correlation.[33−36,45−47]

Adding some exact Hartree−Fock exchange to density functionals by adopting hybrid Hartree−Fock/density functional (HF/DF) methods[33−35,50] has also been demonstrated to give accurate ground-state enthalpies, geometries, and frequencies for an enormous number of molecules,[41,51−56] while retaining the computational economy of pure DFT. One recent exception, a HF/DF study of donor−acceptor complexes between halogen molecules, X_2, and ethylene or ammonia gave poor geometries

and interaction energies.[57] Recent experience shows, however, that halogen anions (X_2^-), representing the limiting case of complete electron transfer to X_2, are particularly difficult for both DFT- and MO-based methods[58,59] and can require coupled pair functional or CASPT2 calculations for accurate description.[59] Thus, it is not surprising that HF/DF methods have difficulty accurately describing this one case of partial electron transfer to form $X_2^{\delta-}$. In contrast, a number of comparative studies of various density functional methods shows the exceptional accuracy of hybrid functionals. It has also been demonstrated that including the exact exchange energy is particularly important for the accurate treatment of transition states.[60−62] For instance, local and gradient corrected density functionals typically underestimate transition state energies for hydrogen abstraction[63−65] and have given artificially shallow minima and negative transition state energies, but hybrid functionals greatly improved the results.[61,65] Numerous studies thus indicate that hybrid functionals give accurate transition state energies for chemical reactions ranging from classical Diels−Alder to hydrogen abstraction.[60,62−69] Since there have been several indications that using hybrid functionals with larger basis sets than 6-31G(d) does not provide any significant accuracy gain in the evaluation of transition state properties,[64,65] we chose to test the relatively inexpensive B3LYP/6-31G(d) method for studying the mechanism of aromatic nitrosations. Moreover, the cationic systems studied here show large interaction energies and substantial geometry changes, indicating strong interactions between subunits. Thus, published work indicates that the B3LYP/6-31G(d) method may provide a balanced treatment of closed- and open-shell systems required to model partial electron-transfer accurately, and it may therefore represent an acceptable compromise between accuracy and computational efficiency. Here, we present tests of the B3LYP/6-31G(d) method for studying the mechanism of benzene and toluene nitrosation by NO^+.

The hybrid B3LYP functional[41,50,70,71] used here employs a weighted sum of Hartree−Fock (E_X^{HF}), local DF, and gradient corrected DF expressions for the exchange and correlation energies as follows

$$E = aE_X^{Slater} + (1-a)E_X^{HF} + b\Delta E_X^{Becke} + cE_C^{LYP} + (1-c)E_C^{VWN}$$

where E_X^{Slater} is Slater's local density functional for exchange,[72] ΔE_X^{Becke} is Becke's gradient-corrected exchange functional,[73] E_C^{VWN} is the local density correlation functional of Vosko, Wilk, and Nuisair,[74] and E_C^{LYP} is the gradient-corrected correlation functional of Lee, Yang, and Parr.[75] The Gaussian split valence plus polarization 6-31G(d) basis set[71,76,77] was used for all DFT calculations reported here. Solely to assist the rapid search for stationary points, preliminary calculations were carried out at the Hartree−Fock (HF) level with the smaller 3-21G basis set, but the results of these calculations are not described in detail. At several points, we note that B3LYP results were checked by using MP2/6-31G(d) and CISD/6-31G(d) calculations.

All calculations were performed by using the GAUSSIAN94 package of programs.[71] Intrinsic reaction coordinate (IRC) calculations using internal coordinates[78−80] were performed to verify that computed transition states were saddle points between reactants and products and atomic charges were estimated using Mulliken population analysis.[81,82] Reported energies include corrections for zero-point energies. Although some workers customarily scale vibrational frequencies to bring them into better agreement with experiment, all frequencies reported here, as well as any quantities derived from vibrational frequencies, are unscaled. If readers wish, frequencies may be multiplied by the scaling factor 0.9614; however, currently available scaling factors were derived for ground-state vibrational frequencies[56] and their use at transitions states is to our knowledge untested.

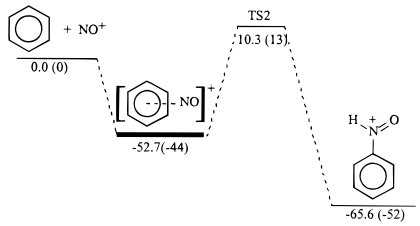

Figure 1. Energy diagram for nitrosation of benzene at the B3LYP/6-31G(d) level of theory. Numbers are the relative energies in kcal/mol. Numbers in parentheses are experimental estimates from ref 19.

TABLE 1: Total Energies in hartrees and ZPE in kcal/mol for Nitrosation of Benzene and Toluene, Calculated by Using the B3LYP/6-31G(d) Method

structure	total energy	ZPE
NO^+	−129.529 786	3.54
C_6H_6	−232.248 651	63.2
C_7H_8	−271.566 648	80.5
A[a]	−361.787 693	68.8
B[a]	−361.802 745	68.7
	Nitrosation of benzene	
$(C_6H_6\cdots NO)^+$	−361.864 608	68.1
TS1		
$C_6H_6NO^+$		
TS2	−361.758 246	64.4
$C_6H_5NOH^+$	−361.883 006	70.6
	Nitrosation of toluene	
$(C_7H_8\cdots NO)^+$	−401.189 193	85.3
o-TS1		
m-TS1		
p-TS1		
o-Wh		
m-Wh		
p-Wh		
o-TS2	−401.086 093	82.0
m-TS2	−401.083 295	81.6
p-TS2	−401.088 864	81.7
o-$C_7H_7NOH^+$	−401.205 789	87.4
m-$C_7H_7NOH^+$	−401.206 523	87.2
p-$C_7H_7NOH^+$	−401.210 648	87.1

[a] Local minima shown in Figure 2.

Mechanism of Nitrosation

The reaction profile for benzene nitrosation computed at the B3LYP/6-31G(d) level of theory is displayed in Figure 1 and total energies of all species are summarized in Table 1. Additional intrinsic reaction coordinate (IRC) calculations at the same level shows that the transition state TS2 is a saddle point connecting the reactants and products indicated. (In addition, the dissociation path for the π-complex has been investigated at the HF level of theory by fixing the distance between the nitrogen atom and the closest carbon atom and reoptimizing all other coordinates.) No barrier has been found for the formation of the π-complex.

In agreement with experimental data, the B3LYP method predicts the formation of a stable π-complex between benzene and NO^+. The calculated structure shown in Figure 2 closely resembles the experimental structures established by X-ray crystallography for π-complexes of various aromatics with NO^+,

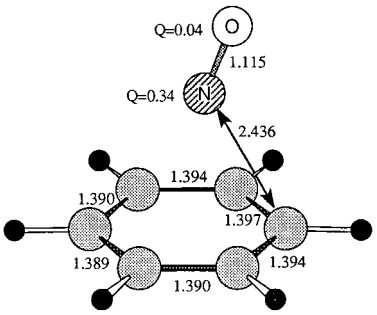

Figure 2. Geometries of the $(C_6H_6\cdots NO)^+$ π-complexes at the B3LYP/6-31G(d) level of theory. Numbers are distances in angstroms; *Q*'s are (positive) atomic charges in au.

indicated in **1**.[5−8] The calculated geometry for (benzene−NO)$^+$ shows the N−O axis tilted approximately 23° off the perpendicular to the ring. Although the shortest calculated N···C distance of 2.44 Å in the (benzene−NO)$^+$ complex is longer than the average N···C distance in hexaalkylbenzene/NO$^+$ complexes,[5,6,8] the calculated distance agrees qualitatively with the average N···C distance of 2.5 Å observed in the X-ray structure of the mesitylene/NO$^+$ complex.[7] The calculated N−O bond length of 1.115 Å in the (benzene−NO)$^+$ complex is slightly less than the experimental N−O distances near 1.13 Å, determined by X-ray diffraction studies of hexamethylbenzene/NO$^+$ complexes,[5,6] and the NO stretching frequency of 2110 cm^{-1} is approximately 14% higher than the experimental frequency of 1849 cm[1], measured for the same hexamethylbenzene/NO$^+$ complex. Since benzene is a poorer electron donor than its hexamethyl derivative, these calculated features are qualitatively consistent with expectations based on EDA theory: the N−O bond distance in (benzene−NO)$^+$ is expected to fall slightly below that in the hexamethylbenzene/NO$^+$ complex and the NO stretching frequency is likewise expected to remain higher. In fact, the calculated N−O distance falls nearly midway between the calculated bond distances of 1.072 Å for NO$^+$ and 1.159 Å for neutral NO and the calculated NO stretching frequency in the π-complex is similarly reduced from the calculated frequency of 2480 cm^{-1} for NO$^+$, but higher than the calculated frequency of 1991 cm^{-1} for NO. These features are all qualitatively consistent with calculated Mulliken atomic charges indicating that 0.62 electron is transferred from benzene to NO$^+$. Calculations thus support the characterization of the π-complex of benzene with NO$^+$ as an EDA complex.

To test reports of multiple intermediates based on MINDO/3 calculations (the most sophisticated analysis of these reactions currently published),[23] we searched for other (benzene−NO)$^+$ π- and σ-complexes. First, the calculated geometry of the π-complex of (benzene−NO)$^+$ shown in Figure 2 has C_1 symmetry and, due to the 6-fold symmetry of benzene, it corresponds to one of six identical π-complexes. Due to the flatness of the potential energy surface in the vicinity of the π-complexes, we were not able to optimize transition states between the six equivalent π-complexes at the B3LYP level of theory. Practically barrierless interconversion of the six π-complexes, indicated by HF/3-21G calculations, will result in effective C_{6v} symmetry.

Next, we located two other benzene complexes with C_1 and C_{2v} symmetry (structures **A** and **B** in Figure 3) identified in earlier MINDO/3 calculations.[23] At the B3LYP level of theory, they represent local minima with energies 48 and 39 kcal/mol above the energy of the π-complex shown in Figure 2, so they are not relevant to the nitrosation mechanism as was previously proposed.[23] Finally, the IRC B3LYP/6-31G(d) calculations

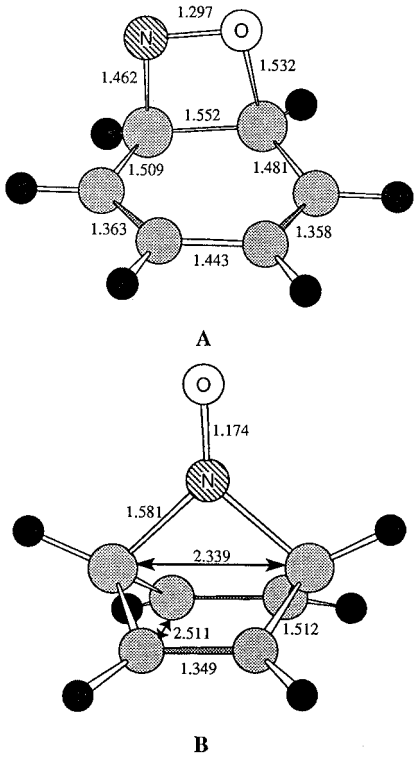

Figure 3. Geometries of local minima **A** (top) and **B** (bottom) at the B3LYP/6-31G(d) level of theory. Numbers are distances in angstroms.

started from the TS2 structure in Figure 1 did not end up in any other local minima.

To further test the B3LYP results, MP2/6-31G(d) and CISD/6-31G(d) calculations were performed, starting from the geometry of a Wheland σ-complex. In the MP2 calculations, the system showed no energy minimum at a σ-complex geometry, but instead moved to the π-complex's geometry. CISD calculations, however, indicate a marginally stable σ-complex very similar to the Wheland intermediate proposed in aromatic nitrations.[9,18] At the B3LYP/6-31G(d) level of theory the reaction barrier in Figure 1 was found to be 10.3 kcal/mol above the dissociation limit, compared with experimental estimates of 13 kcal/mol. Moreover, the B3LYP method overestimates the stabilities (relative to reactants) of the π-complex, 52.7 kcal/mol, and N-protonated nitrosobenzene, 65.6 kcal/mol, as compared to the corresponding experimental, gas-phase estimates of 44 ± 5 and 52 ± 7 kcal/mol, respectively.[3]

Although the relatively large CISD/6-31G(d) energy barrier for converting the σ-complex to an N-protonated nitrosobenzene apparently support the accepted nitrosation mechansim in solvent (see Appendix) involving rate-limiting deprotonation of a σ-complex, B3LYP/6-31G(d) and MP2/6-31G(d) calculations suggest a new alternative—the rate-limiting conversion of the π-complex to the N-protonated nitroso-derivative. Given the uncertanties in computed values of reaction barriers, as well as in the rate of proton transfer, it appears plausible that the alternative mechanism can operate alone or be complimentary to the generally accepted mechanism.

The geometries and atomic charges for the transition state and N-protonated nitrosobenzene intermediate determined from B3LYP analysis of the alternative mechanism are shown in Figure 4. The structure of the transition state corresponds to the nitroso group inserting into the aromatic C−H bond and involves primarily hydrogen migration from the aromatic carbon to the nitrogen of N-protonated nitrosobenzene. The preeminence of hydrogen migration in the transition state is reminiscent

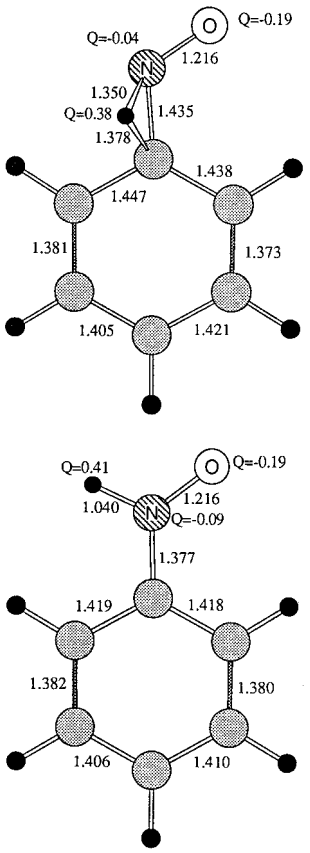

Figure 4. Geometries of transition state (top) and N-protonated nitrosobenzene (bottom) at the B3LYP/6-31G(d) levels of theory. Numbers are distances in angstroms; Q's are (positive) atomic charges in au.

of the migratory insertion of carbon monoxide into metal−carbon bonds[83] and is supported by the analysis of motion along the imaginary vibrational mode. This mode's frequency is very large, 1870i cm^{-1}, and the corresponding reduced mass of 1.12 amu is very close to that of the hydrogen atom.

The significance of hydrogen migration in the B3LYP transition state for converting the π-complex to an N-protonated nitrosobenzene provides an opportunity to test the plausibility of the alternative mechanism by calculating the kinetic isotope effect. We therefore computed partition functions and vibrational frequencies for the deuterium substituted π-complex and TS2. The ratio of rate constants can be expressed as

$$\frac{k_{2,H}}{k_{2,D}} = \frac{\kappa_H}{\kappa_D}\exp\left(\frac{\Delta G_D^{\ddagger} - \Delta G_H^{\ddagger}}{RT}\right) \quad (1)$$

Here κ is a transmission coefficient, $\Delta G^{\ddagger}$ is the activation free energy, and indices H and D denote nonsubstituted and deuterium substituted substrates, respectively. Transmission coefficients were computed from the expression proposed by Bell[84]

$$\kappa = 1 + \frac{u^2}{24} + \frac{7u^2}{5760} \qquad \text{where} \qquad u = \frac{h|\nu|}{k_B T} \quad (2)$$

and ν is the imaginary frequency at the transition state. At 325 K the kinetic isotope effect (eq 6) for benzene nitrosation was calculated to be 11.5, where the ratio of preexponentials is estimated as $\kappa_H/\kappa_D = 2.1$. The calculated k_H/k_D agrees qualitatively with the experimental value of 8.5, obtained at 325 K for nitrosation of benzene in sulfuric acid (rates were measured to within approximately ±20%).[19]

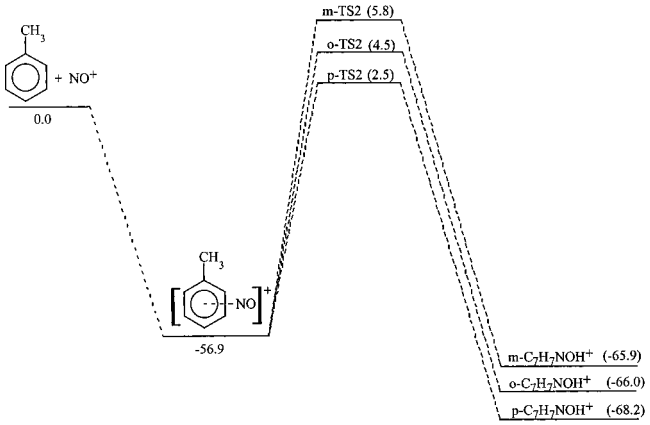

Figure 5. Energy diagram for nitrosation of toluene at the B3LYP/6-31G(d) level of theory. Numbers are the relative energies in kcal/mol.

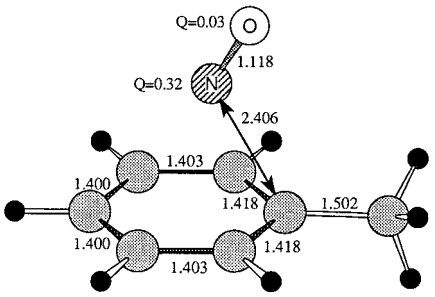

Figure 6. Geometry of the $(C_7H_8\cdots NO)^+$ π-complex at the B3LYP/6-31G(d) level of theory. Numbers are distances in Å; Q's are (positive) atomic charges in au.

To further test the validity and generality of the alternative reaction scheme for gas-phase nitrosation suggested by B3LYP calculations, the reaction scheme for toluene nitrosation was also computed at the B3LYP/6-31G(d) level of theory and is shown in Figure 5. Total and zero-point energies of all species are summarized in Table 1. Figure 5 was generated by optimizing the π-complex geometry three times at the HF level of theory, starting from the previously identified geometry of the $(C_6H_6\cdots NO)^+$ π-complex but with a CH_3 group substituted in three different positions. All three calculations converged to the same geometry of the $(C_7H_8\cdots NO)^+$ π-complex, which was subsequently reoptimized at the B3LYP/6-31G(d) level of theory. The B3LYP/6-31G(d) structure is displayed in Figure 6. In this complex the $NO^{\delta+}$ molecule is positioned above the aromatic plane with its N−O bond titled off the perpendicular to the aromatic ring by 32 degrees with the closest N···C distance of 2.41 Å, slightly smaller than corresponding distance in the $(C_6H_6\cdots NO)^+$ π-complex. The calculated NO stretching frequency for the (toluene···NO)$^+$ π-complex (2087 cm^{-1}) is also slightly lower than that of the $(C_6H_6\cdots NO)^+$ π-complex, indicating greater charge transfer from toluene to NO^+ in the toluene complex. The greater reactivity of toluene as compared to benzene also receives support from the more extensive charge-transfer evident in the toluene complex. For the toluene complex, Mulliken population analysis[81,82] shows 0.65 electron is transferred compared to 0.62 electron for the benzene complex, the NO bond is slightly longer, 1.118 Å as compared to 1.115 Å, and the dissociation energy is larger, 56.9 kcal/mol as compared to 52.7 kcal/mol.

The B3LYP barriers for rearrangement of the π-complex into the N-protonated nitrosotoluene (denoted as *o*-TS2, *m*-TS2, and

p-TS2 in Table 1 and Figure 5) vary from 2.5 kcal/mol for para-substitution to 5.8 kcal/mol for meta- substitution with respect to the π-complex dissociation limit, so all calculated barriers are lower than the corresponding barrier for benzene nitrosation. These results are in qualitative agreement with the experimental observation of higher reactivity of toluene toward the nitrosation.[19] The imaginary frequencies were found to be 1811i, 1841i, and 1912i cm^{-1} for *o*-TS2, *m*-TS2, and *p*-TS2, respectively, with associated reduced masses being close to 1.2 amu in all three cases. Thus, similar to the benzene nitrosation, B3LYP transition states for toluene nitrosation are due to migratory insertion of nitrogen into the aromatic C−H bond.

A kinetic analysis similar to that carried out for benzene nitrosation has also been accomplished for toluene. From eq 4 we computed the effective rate constant as the sum of three channels (ortho-, meta-, and para-) to be 5×10^8 cm^3 mol^{-1} s^{-1}. This figure is 5 orders of magnitude larger than the one computed for benzene nitrosation, in contrast to the experimentally observed[19] rate enhancement of approximately 100. The large quantitative discrepancy might be due to an improper mechanism implied by B3LYP calculations, inaccuracies in activation energies calculated by using the B3LYP/6-31G(d) method (along with a relatively low-temperature kinetic analysis), or solvent effects. The ordering of barrier heights for nitrosation of toluene in the ortho-, meta-, and para-positions (Figure 5) is in qualitative agreement with typically observed regioselectivity in substitution reactions.[85] If reaction 2 is the rate-limiting step, then the ratio of regioisomers can be calculated from the ratio of the corresponding rate constants for transformation of the π-complex into the N-protonated nitrosotoluene isomers. At the B3LYP level of theory the ortho-:meta-:para-ratio was computed to be 2:0.4:98. If proton loss is the rate-limiting step, the ratio of isomers will reflect the relative thermodynamic stabilities of ortho-, meta-, and para-substituted N-protonated nitrosotoluenes. Based on the B3LYP/6−31(d) results this ratio was calculated to be 0.4:0.8:99. In both cases nitrosation takes place mainly at the para-position as it was observed for other, more reactive aromatic substrates.[86]

The present results indicate that it would not be easy to distinguish between different rate-limiting steps, conversion of the π-complex or deprotonation of an N-protonated nitrosoaromatic, based on measurements of the product's isomeric composition. The above discussion of isotope effects also implies that a substrate isotopic substitution is unable to distinguish unambiguously between these two different rate-limiting steps. A solvent isotopic substitution, on the other hand, should lead to an isotope effect if proton transfer is rate limiting, so observation of a significant solvent isotope effect would disprove the possibility that insertion is the rate-limiting step.[87] In that case, the rate-limiting step might involve deprotonation of a Wheland intermediate (unlikely, on the basis of the measured substrate isotope effect of $k_H/k_D = 8.5$[19]) or of an N-protonated nitrosoaromatic. To address the larger question of the existence of Wheland σ-complex intermediates vs N-protonated nitroso intermediates apparently requires their experimental detection or higher level calculations.

Finally, because the π-complex in Scheme 1 closely resembles a radical pair, regioselectivity and the unpaired electron densities on atoms of aromatic radical cations may be correlated.[88] To test this proposal, we used Mulliken population analysis[81,82] to compute atomic spin densities on atoms of $C_7H_8^{\bullet+}$ and $C_6H_6^{\bullet+}$ radicals whose structures were optimized at the B3LYP/6-31G(d) level of theory. Although a linear correlation appears between spin densities and Gibbs free energy barriers for *o*-, *p*-, and *m*-toluene, the corresponding data point for benzene appears far from the correlation line.

Summary

This contribution reports the highest level calculations published to date describing the nitrosation of benzene and toluene, resolves several issues, and raises some intriguing questions. B3LYP calculations indicate the applicability of hybrid Hartree−Fock/density functionals for modeling the structures and vibrations of electron donor−acceptor complexes, supports the intermediacy of donor−acceptor π-complexes in gas-phase aromatic nitrosations of benzene and toluene, and shows that several additional intermediates suggested by MINDO/3 calculations[23] are kinetically irrelevant. Reaction energetics agree with experiment only approximately, so a more accurate quantum chemical technique than the B3LYP/6-31G(d) method appears necessary achieve agreement between calculated and experimental relative energies and reaction rates.

Strongly bonded (benzene−NO)$^+$ and (toluene−NO)$^+$ π-complexes were identified as intermediates in both nitrosation reactions and their calculated structures agree well with available experimental data. The extent of electron transfer from the aromatic to NO^+ is greater than 0.6 electron in each π-complex, confirming their donor−acceptor nature and supporting the characterization of the reactions as oxidative aromatic substitutions. According to B3LYP calculations (supported by the MP2/6-31G(d) method), π-complex intermediates subsequently rearrange to N-protonated nitroso-derivatives by a migratory insertion of nitrogen into the aromatic C−H bond. The transition state for the migratory insertion involves substantial hydrogen migration and displays a calculated deuterium kinetic isotope effect of $k_H/k_D = 11.5$ for benzene, in qualitative agreement with the experimentally measured isotope effect of 8.5 (rates were measured only to within ±20%).[19] Kinetic analysis of proton loss from N-protonated nitroso-derivatives indicates that deprotonation would not be the rate-limiting step as was previously proposed on the basis of the observed kinetic isotope effects and analogy with aromatic nitrations.[12,17,19,86,89,90] Finally, B3LYP calculations indicate that nitrosation of toluene leads mostly to the para-substituted derivative, in agreement with experimental data.[19] The ratio of ortho-, meta-, and para-isomers was found to be relatively insensitive to the conditions of nitrosation.

Contrary to prevailing assumptions for nitrosation in solvents (expressed in Scheme 1), stable Wheland σ-complexes were not found at the B3LYP/6-31G(d) or MP2/6-31G(d) levels of calculation; however, σ-complexes appeared as intermediates in CISD/6-31G(d) calculations of the reaction. Thus, the mechanistic alternative suggested by B3LYP amd MP2 calculations is uncertain and should be tested by using larger basis sets and higher level computational methods that model nondynamical and dynamical correlation well. We also note that present analyses are based on gas-phase energetics and qualitative analogies, so that thorough theoretical and experimental investigations of the various possible proton-transfer processes should also be done to answer the several outstanding questions concerning the mechanism of aromatic nitrosations.

Acknowledgment. Supercomputer time at the National Center for Supercomputing Applications and the Cornell Theory Center, provided through the NSF/MetaCenter Allocations Committee, is gratefully acknowledged. The Cornell Theory Center receives major funding from the NSF and New York State. Additional funding for the Cornell Theory Center comes

from ARPA, the National Institutes of Health, IBM Corporation, and other members of the center's Corporate Research Institute. Additional supercomputer time at the University of Oklahoma was made possible by support from the University of Oklahoma, IBM Corporation, and Silicon Graphics, Inc. We are grateful to Professor George Richter-Addo for helpful discussions and to Susan E. Walden for carefully reading the manuscript.

Appendix. Nitrosation Kinetics

The overall effective rate constant for benzene nitrosation can be expressed by using the steady-state approximation for Scheme 2 as

$$k_{\text{eff}} = \frac{k_1 k_2 k_3[\text{B}]}{k_{-1}k_{-2} + (k_{-1} + k_2)k_3[\text{B}]}, \quad \text{where} \qquad k_{-1} = \frac{k_1}{K_{\text{eq1}}} \tag{A.1}$$

where k_i and k_{-i} are the rate constants for ith reaction in the forward and reverse directions, respectively, [B] denotes the concentration of base (see Scheme 2), and K_{eq1} is the equilibrium constant for the first step. The relation between forward and reverse rate constants is due to the principle of microscopic reversibility. The rate constant for the barrierless formation of the π-complex k_1 can be estimated for the gas phase from Langevin theory[91] and for solution from the Stokes−Einstein relation[92] using the following expressions

$$k_1(\text{gas}) = 2\pi\sqrt{\frac{e^2\alpha}{\mu}} \qquad k_1(\text{solvent}) = \frac{8RT}{3\eta} \tag{A.2}$$

Here e is the electron charge, α is molecular polarizibility, μ is reduced mass, η is viscosity, R is the universal gas constant, and T is absolute temperature. In the gas phase, k_1 is about 3×10^{14} cm^3 mol^{-1} s^{-1} and in 90% sulfuric acid, k_1 is approximately 3×10^{11} cm^3 mol^{-1} s^{-1} at 300 K. The decrease of the rate constant in solution is due to a 5 kcal/mol diffusion barrier.[92] From the principle of detailed balancing, the gas-phase rate constant for dissociation k_{-1} was computed to be 1.5×10^{-22} s^{-1}. The values of k_2 and k_{-2}, were calculated from a nonvariational transition state theory[93] (TST) expression

$$k_{\text{TST}} = \frac{k_{\text{B}}T}{h}\exp\left(-\frac{\Delta G_0^{\ddagger}}{RT}\right) \tag{A.3}$$

where k_{B} is the Boltzmann's constant, h is Planck's constant, and $\Delta G_0^{\ddagger}$ is the Gibbs activation free energy in the standard state. From the B3LYP/6-31G(d) results, the values of k_2 and k_{-2} were found to be 2×10^{-34} s^{-1} and 2×10^{-40} s^{-1}, respectively. There has been no direct measurement of the rate of the product forming step, abstraction of a proton, and even the chemical nature of the abstracting species remains uncertain. This problem is outside the scope of the present study, yet for the sake of qualitative discussion some speculations can be made. Let us consider two possible situations, a fast proton-transfer step and rate-limiting proton transfer. In the first case, eq A.1 reduces to the expression

$$k_{\text{eff}} = \frac{k_1 k_2}{k_{-1} + k_2} \tag{A.4}$$

Substituting computed rate constants into eq A.4 yields an effective rate constant on the order of 10^3 cm^3 mol^{-1} s^{-1}. This figure is somewhat larger than experimental values of 0.4 and 15 cm^3 mol^{-1} s^{-1} for benzene nitrosation in concentrated $HClO_4$ and H_2SO_4 acids, respectively.[19] The discrepancy might be due to the underestimation of energy barriers at the B3LYP level and/or due to the increase of barrier heights in solution. The latter explanation is quite plausible since the small NO^+ ion should be stabilized in solution to a larger degree than the transition state. Comparing the effective rate constant with the collisional limit of 10^{15} cm^3 mol^{-1} s^{-1} one might deduce that NO^+ is about 10^{12} (or 10^{14} as it was deduced from experimental data[19]) times less reactive than NO_2^+, where the latter is assumed to react at the encounter controlled rate. It should be pointed out that such a comparison of relative reactivities of NO^+ and NO_2^+, though important for practical applications, is theoretically meaningless since it is based on the comparison of the overall reaction rates for two different multistep mechanisms.

It has been reported that the rate of nitrosation is 8.5 times slower for deuterium substituted benzene than for nonsubstituted benzene. This kinetic isotope effect has been explained as a consequence of rate-limiting proton transfer. If this is the case, eq A.3 of the appendix reduces to the following expression

$$k_{\text{eff}} = K_{\text{eq1}}K_{\text{eq2}}k_3[\text{B}] \tag{A.5}$$

where K_{eq2} is the equilibrium constant for the second step. Note that this expression is valid if $k_3[\text{B}] < k_{-2}$ ($\approx 10^{-40}$ s^{-1}). Regardless of the actual mechanism of proton transfer, which might involve several elementary reaction steps, the preexponential factor in solution at 300 K should be about 10^{11} cm^3 mol^{-1} s^{-1}. This figure is from eq 2 and already includes the diffusion barrier. Then, assuming that base B is a water molecule in 90% acid solution, one can estimate a lower bound for the proton-transfer barrier as about 70 kcal/mol. Since B3LYP/6-31G(d) overestimates the barrier for the reverse of reaction 2 by 11 kcal/mol (Figure 1), more realistic estimates for the barrier to proton transfer might be about 60 kcal/mol. The latter estimate still seems too large as compared to the 40 kcal/mol barrier computed for proton transfer from NH_4^+ to H_2O.[94] While the resolution of this contradiction awaits future investigations of proton transfer from protonated aromatics, this paper offers an alternative explanation for the kinetic isotope effect.

A similar analysis using eq A.1 can be carried out for nitrosation through the Wheland σ-complex. Let us denote the rate constant for transformation of the π-complex into a σ-complex as k_2' and the rate of σ-complex deprotonation as k_3'. From UHF data we estimated k_2' as 10^4 s^{-1} and the reverse rate constant k_{-2}' as 10^{13} s^{-1}. As discussed above, proton transfer will be the rate-limiting step if $k_3'[\text{B}] < k_{-2}'$. Assuming again that base B is a water molecule in 90% acid solution, a lower bound for the proton-transfer barrier was estimated as 6 kcal/mol. If the barrier for proton transfer is too large, the σ-complex will be transformed into an N-protonated nitrosobenzene rather then deprotonated. The transformation rate of the σ-complex into N-protonated nitrosobenzene k_4 is on the order of 10^{-25} s^{-1}. The inequality $k_3'[\text{B}] > k_{-4}$ gives an upper bound for the proton transfer barrier of approximately 45 kcal/mol. Thus, within a wide range of barriers, 6−45 kcal/mol, (and/or a wide range of concentration of B) proton transfer from the σ-complex will be the rate-limiting step in nitrosation. However, the slow overall nitrosation rate evident from experiments indicates an effective barrier of about 15 kcal/mol and places a much more restrictive requirement on the proton-transfer rate. Substituting K_{eq1}, K_{eq2}', and $k_3'[\text{B}]$ in A.5 and equating it with the experimental effective nitrosation rate of benzene, one obtains an estimate for the proton transfer barrier of 35 kcal/mol, just 10 kcal/mol below the upper bound required to ensure that proton transfer is the rate-limiting step (45 kcal/mol). Keeping

in mind the rather limited accuracy of UHF calculations and the fact that TS2 is significantly lowered at the B3LYP level, it seems possible that k_3'[B] and k_{-4} might have similar magnitudes and the two different mechanisms will operate simultaneously.

Supporting Information Available: Tables containing Cartesian coordinates for structures of species listed in Table 1, calculated at the B3LYP/6-31G(d) level. Supporting Information is available free of charge via the Internet at http://pubs.acs.org.

References and Notes

(1) Wheeler, R. A.; Skokov, S. *Abstracts of Papers*, March 30, 1998; 215th National Meeting of the American Chemical Society, **1998**, *215*, COMP 027.

(2) Allan, Z. J.; Podstata, J.; Snobl, D.; Jarkovsky, J. *Collect. Czech. Chem. Commun.* **1967**, *32*, 1449−1461.

(3) Reents, W. D.; Freiser, B. S. *J. Am. Chem. Soc.* **1980**, *102*, 271−276.

(4) Reents, W. D.; Freiser, B. S. *J. Am. Chem. Soc.* **1981**, *103*, 2791−2797.

(5) Brownstein, S.; Gabe, E.; Lee, F.; Tan, L. *J. Chem. Soc., Chem. Commun.* **1984**, 1566−1568.

(6) Brownstein, S.; Gabe, E.; Lee, F.; Piotrowski, A. *Can. J. Chem.* **1986**, *64*, 1661−1667.

(7) Kim, E. K.; Kochi, J. K. *J. Am. Chem. Soc.* **1991**, *113*, 4962−4974.

(8) Rathore, R.; Lindeman, S. V.; Kochi, J. K. *J. Am. Chem. Soc.* **1997**, *119*, 9393−9404.

(9) Taylor, R. *Electrophilic Aromatic Substitution*; Wiley: New York, 1990.

(10) Chupakhin, O. N.; Charushin, V. N.; van der Plas, H. C. *Nucleophilic Aromatic Substitution of Hydrogen*; Academic: San Diego, 1994.

(11) Rossi, R. A.; de Rossi, R. H. *Aromatic Substitution by the $S_{RN}1$ Mechanism*; American Chemical Society: Washington, DC, 1983.

(12) Bosch, E.; Kochi, J. K. *J. Org. Chem.* **1994**, *59*, 5573−5586.

(13) Kochi, J. K. *Acta Chem. Scand.* **1990**, *44*, 409−432.

(14) Laane, J.; Ohlsen, J. R. *Prog. Inorg. Chem.* **1980**, *27*, 465−513.

(15) Keck, D. B.; Hause, C. D. *J. Mol. Spectrosc.* **1968**, *26*, 163−174.

(16) Loeppky, R. N., Michejda, C. J., Eds. *Nitrosamines and Related N−Nitroso Compounds*; American Chemical Society: Washington, DC, 1994; Vol. 553.

(17) Williams, D. L. H. *Nitrosation*; Cambridge University Press: New York, 1988.

(18) Olah, G. A.; Malhotra, R.; Narang, S. C. *Nitration. Methods and Mechanisms*; VCH: New York, 1989.

(19) Challis, B. C.; Higgins, R. J.; Lawson, A. J. *J. Chem. Soc., Perkin Trans. 2* **1972**, 1831−1836.

(20) Raghavachari, K.; Reents, W. D.; Haddon, R. C. *J. Comput. Chem.* **1986**, *7*, 265−273.

(21) Minyaev, R. M.; Kletskii, M. E.; Minkin, V. I. *Russ. J. Org. Chem.* **1987**, *23*, 2213−225.

(22) Borodkin, G. I.; Elanov, I. R.; Podryvanov, V. A.; Shakirov, M. M.; Shubin, V. G. *J. Am. Chem. Soc.* **1996**, *117*, 12863−12864.

(23) Minkin, V. I.; Minyaev, R. M.; Yudilevich, I. A.; Kletskii, M. E. *Russian J. Org. Chem.* **1985**, *21*, 842−853.

(24) Mok, D. K. W.; Neumann, R.; Handy, N. C. *J. Phys. Chem.* **1996**, *100*, 6225−6230 and references therein.

(25) Gross, E. K. U.; Petersilka, M.; Grabo, T. Conventional quantum chemical correlation energy versus density-functional correlation energy. In *Chemical Applications of Density-Functional Theory*; Laird, B. B., Ross, R. B., Ziegler, T., Eds. American Chemical Society: Washington, DC, 1996; Vol. 629, pp 42−53.

(26) McWeeny, R. W. Present status of the correlation problem. In *The New World of Quantum Chemistry*; Pullman, B., Parr, R., Eds.; D. Reidel: Dordrecht, 1976; pp 3−31.

(27) Chipman, D. M. *Theor. Chim. Acta* **1992**, *82*, 93−115.

(28) Roos, B. O. *Adv. Chem. Phys.* **1987**, *69*, 399−445.

(29) Shepard, R. *Adv. Chem. Phys.* **1987**, *69*, 63−200 and references therein.

(30) Wolinski, K.; Sellers, H. L.; Pulay, P. *Chem. Phys. Lett.* **1987**, *140*, 225−231.

(31) Wolinski, K.; Pulay, P. *J. Chem. Phys.* **1990**, *94*, 3647−3659.

(32) Andersson, K.; Roos, B. O. Multiconfiguration second-order perturbation theory. In *Modern Electronic Structure Theory, Part I*; Yarkony, D. R., Ed.; World Scientific: Singapore, 1995; Vol. 2, pp 55−109.

(33) Kohn, W.; Becke, A. D.; Parr, R. G. *J. Phys. Chem.* **1996**, *100*, 12974−12980.

(34) Becke, A. D. Exchange-correlation approximations in density functional theory. In *Modern Electronic Structure Theory, Part II*; Yarkony, D. R., Ed.; World Scientific: Singapore, 1995; Vol. 2, pp 1022−1046.

(35) Ernzerhof, M.; Perdew, J. P.; Burke, K. *Topics Curr. Chem.* **1996**, *180*, 1−30.

(36) Parr, R. G.; Yang, W. *Density-Functional Theory of Atoms and Molecules*; Oxford University: New York, 1989.

(37) Ziegler, T. *Chem. Rev.* **1991**, *91*, 651−667.

(38) Dreizler, R. M.; Gross, E. K. V. *Density Functional Theory*; Springer: Berlin, 1990.

(39) Parr, R. G.; Yang, W. *Annu. Rev. Phys. Chem.* **1995**, *46*, 701−728.

(40) Schlegel, H. B.; Frisch, M. J. Computational bottlenecks in molecular orbital calculations. In *Theoretical and Computational Models for Organic Chemistry*; Formosinho, S. J., Csizmadia, I. G., Arnaut, L. G., Eds.; Kluwer: Dordrecht, 1991; pp 5−33.

(41) Foresman, J. B.; Frisch, A. *Exploring Chemistry with Electronic Structure Methods*, 2nd ed.; Gaussian, Inc.: Pittsburgh, PA, 1996.

(42) Engels, B.; Eriksson, L. A.; Lunell, S. *Adv. Quantum Chem.* **1996**, *27*, 297−369.

(43) Malkin, V. G.; Malkina, O. L.; Eriksson, L. A.; Salahub, D. R. The calculation of NMR and ESR spectroscopy parameters using density functional theory. In *Modern Density Functional Theory: A Tool for Chemistry*; Seminario, J. M., Politzer, P., Eds.; Elsevier Science B. V.: Dordrecht, 1995; Vol. 2, pp 273−347.

(44) Barone, V. *Theor. Chim. Acta* **1995**, *91*, 113−128.

(45) Andzelm, J.; Wimmer, E. *J. Chem. Phys.* **1992**, *96*, 1280−1303.

(46) Johnson, B. G.; Gill, P. M. W.; Pople, J. A. *J. Chem. Phys.* **1993**, *98*, 5612−5626.

(47) Laming, G.; Handy, N. C.; Amos, R. D. *Mol. Phys.* **1993**, *80*, 1121−1134.

(48) Murray, C. W.; Handy, N. C.; Amos, R. D. *J. Chem. Phys.* **1993**, *98*, 7145−7151.

(49) Cramer, C. J.; Dulles, F. J.; Storer, J. W.; Worthington, S. E. *Chem. Phys. Lett.* **1994**, *218*, 387−394.

(50) Becke, A. D. *J. Chem. Phys* **1993**, *98*, 5648−5652.

(51) Martell, J. M.; Goddard, J. D.; Eriksson, L. A. *J. Phys. Chem. A* **1997**, *101*, 1927−1934.

(52) Mole, S. J.; Zhou, X.; Liu, R. *J. Phys. Chem.* **1996**, *100*, 14665−14671.

(53) Bauschlicher, C. W.; Partridge, H. *Chem. Phys. Lett.* **1995**, *240*, 533−540.

(54) Hay, P. J. *J. Phys. Chem.* **1996**, *100*, 5−8.

(55) Rauhut, G.; Pulay, P. *J. Phys. Chem.* **1995**, *99*, 3−3100.

(56) Scott, A. P.; Radom, L. *J. Phys. Chem.* **1996**, *100*, 16502−16513.

(57) Ruiz, E.; Salahub, D. R.; Vela, A. *J. Phys. Chem.* **1996**, *100*, 12265−12276.

(58) Raymond, K. S.; Wheeler, R. A. *J. Comput. Chem.* **1999**, *20*, 207−216.

(59) Eberson, L.; Gonzalez-Luque, R.; Lorentzon, J.; Merchan, M.; Roos, B. O. *J. Am. Chem. Soc.* **1993**, *115*, 2898−2902.

(60) Johnson, B. G.; Gonzales, C. A.; Gill, P. M. W.; Pople, J. A. *Chem. Phys. Lett.* **1994**, *221*, 100−108.

(61) Baker, J.; Andzelm, J.; Muir, M.; Taylor, P. R. *Chem. Phys. Lett.* **1995**, *236*, 53.

(62) Wiest, O.; Houk, K. N. *Top. Curr. Chem.* **1996**, *183*, 1−24.

(63) Baker, J.; Muir, M.; Andzelm, J. *J. Chem. Phys.* **1994**, *102*, 2063−2079.

(64) Durant, J. L. *Chem. Phys. Lett.* **1996**, *256*, 595−602.

(65) Skokov, S.; Wheeler, R. A. *Chem. Phys. Lett.* **1997**, *271*, 251−258.

(66) Baker, J.; Muir, M.; Andzelm, J.; Scheiner, A. Hybrid Hartree−Fock Density-functionals theory functionals: The adiabatic connection methodol. In *Chemical Applications of Density-Functional Theory*; Laird, B. B., Ross, R. B., Ziegler, T., Eds.; American Chemical Society: Washington, DC, 1996; Vol. 629, pp 342−367.

(67) Goldstein, E.; Beno, B.; Houk, K. N. *J. Am. Chem. Soc.* **1996**, *118*, 6036−6043.

(68) Jursic, B.; Zdravkovski, Z. *J. Chem. Soc., Perkin Trans. 2* **1995**, 1223−1226.

(69) Basch, H.; Hoz, S. *J. Phys. Chem. A* **1997**, *101*, 4416−4431.

(70) Stephens, P. J.; Devlin, F. J.; Chabalowski, C. F.; Frisch, M. J. *J. Phys. Chem.* **1994**, *98*, 11623−11627.

(71) Frisch, M. J.; Trucks, G. W.; Schlegel, H. B.; Gill, P. M. W.; Johnson, B. G.; Robb, M. A.; Cheeseman, J. R.; Keith, T. A.; Petersson, G. A.; Montgomery, J. A.; Raghavachari, K.; Al-Laham, M. A.; Zakrzewski, V. G.; Ortiz, J. V.; Foresman, J. B.; Cioslowski, J.; Stefanov, B. B.; Nanayakkara, A.; Challacombe, M.; Peng, C. Y.; Ayala, P. Y.; Chen, W.; Wong, M. W.; Andres, J. L.; Replogle, E. S.; Gomperts, R.; Martin, R. L.; Fox, D. J.; Binkley, J. S.; Defrees, D. J.; Baker, J.; Stewart, J. J. P.; Head-Gordon, M.; Gonzalez, C.; Pople, J. A. *GAUSSIAN94*, Revision B.3; Gaussian, Inc.: Pittsburgh, 1995.

(72) Slater, J. C. *Quantum Theory of Molecules and Solids*; McGraw-Hill: New York, 1974; Vol. 4.
(73) Becke, A. D. *Phys. Rev. A* **1988**, *38*, 3098−3100.
(74) Vosko, S. H.; Wilk, L.; Nusair, M. *Can. J. Phys.* **1980**, *58*, 1200−1211.
(75) Lee, C.; Yang, W.; Parr, R. G. *Phys. Rev. B* **1988**, *37*, 785−789.
(76) Hehre, W. J.; Radom, L.; Schleyer, P. v. R.; Pople, J. A. *Ab Initio Molecular Orbital Theory*; John Wiley & Sons: New York, 1986.
(77) Helgaker, T.; Taylor, P. R. Gaussian basis sets and molecular integrals. In *Modern Electronic Structure Theory, Part II*; Yarkony, D. R., Ed.; World Scientific: Singapore, 1995; Vol. 2, pp 725−856.
(78) Gonzalez, C.; McDouall, J. J. W.; Schlegel, H. B. *J. Phys. Chem.* **1990**, *94*, 7467.
(79) Gonzalez, C.; Schlegel, H. B. *J. Chem. Phys.* **1989**, *90*, 2154−2161.
(80) Fukui, K. *Acc. Chem. Res.* **1981**, *14*, 363−368.
(81) Mulliken, R. S. *J. Chem. Phys.* **1955**, *23*, 1833−1840.
(82) Mulliken, R. S.; Ermler, W. C. *Diatomic Molecules*; Academic: New York, 1977.
(83) Collman, J. P.; Hegedus, L. S.; Norton, J. R.; Finke, R. G. *Principles and Applications of Organotransition Metal Chemistry*; University Science Books: Mill Valley, CA, 1987, Section 6.1c.
(84) Bell, R. P. *Trans. Faraday Soc.* **1959**, *55*, 1−4.
(85) Schofield, K. *Aromatic Nitration*; Cambridge University Press: New York, 1980.
(86) Challis, B. C.; Lawson, A. J. *J. Chem. Soc. B* **1971**, 770−775.
(87) Isaacs, N. S. *Physical Organic Chemistry*, 2nd ed.; Longman Scientific & Technical: Essex, 1995; pp 307−314.
(88) Pederson, E. B.; Peterson, T. E.; Torssell, K.; Lawesson, S.-O. *Tetrahedron* **1973**, *29*, 579−584.
(89) Challis, B. C.; Lawson, A. J. *J. Chem. Soc., Chem. Commun.* **1968**, 818−819.
(90) Challis, B. C.; Higgins, R. J. *J. Chem. Soc., Perkin 2* **1973**, 1597−1604.
(91) Giomousis, G.; Stevenson, D. P. *J. Chem. Phys.* **1958**, *29*, 294−299.
(92) Ridd, J. H. *Adv. Phys. Org. Chem.* **1978**, *16*, 1−49.
(93) Robinson, P. J.; Holbrook, K. A. *Unimolecular Reactions*; The Stonebridge Press: Bristol, UK, 1970.
(94) Jaroszewski, L.; Lesyng, B.; McCammon, J. A. *J. Mol. Structure* **1993**, *283*, 57.